This article was downloaded by: *[Fox, Jefferson M.]*
On: *20 July 2010*
Access details: *Access Details: [subscription number 924595482]*
Publisher *Taylor & Francis*
Informa Ltd Registered in England and Wales Registered Number: 1072954 Registered office: Mortimer House, 37-41 Mortimer Street, London W1T 3JH, UK

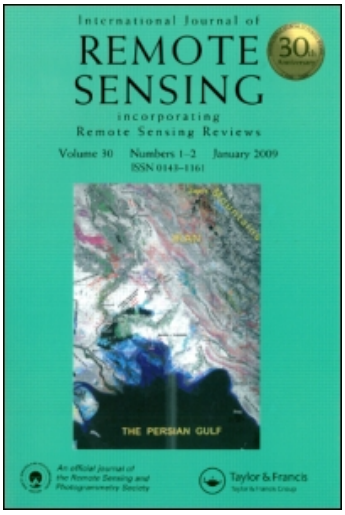

International Journal of Remote Sensing
Publication details, including instructions for authors and subscription information:
http://www.informaworld.com/smpp/title~content=t713722504

Topographic normalization for improving vegetation classification in a mountainous watershed in Northern Thailand

Lan Cuo[a]; John B. Vogler[b]; Jefferson M. Fox[c]
[a] Australia Commonwealth Scientific and Industrial Research, Organization (CSIRO), Highett, Australia [b] Department of Anthropology, University of Hawaii at Manoa, USA [c] East-West Center, Honolulu, Hawaii, USA

Online publication date: 20 July 2010

To cite this Article Cuo, Lan , Vogler, John B. and Fox, Jefferson M.(2010) 'Topographic normalization for improving vegetation classification in a mountainous watershed in Northern Thailand', International Journal of Remote Sensing, 31: 11, 3037 — 3050
To link to this Article: DOI: 10.1080/01431160903154333
URL: http://dx.doi.org/10.1080/01431160903154333

PLEASE SCROLL DOWN FOR ARTICLE

Full terms and conditions of use: http://www.informaworld.com/terms-and-conditions-of-access.pdf

This article may be used for research, teaching and private study purposes. Any substantial or systematic reproduction, re-distribution, re-selling, loan or sub-licensing, systematic supply or distribution in any form to anyone is expressly forbidden.

The publisher does not give any warranty express or implied or make any representation that the contents will be complete or accurate or up to date. The accuracy of any instructions, formulae and drug doses should be independently verified with primary sources. The publisher shall not be liable for any loss, actions, claims, proceedings, demand or costs or damages whatsoever or howsoever caused arising directly or indirectly in connection with or arising out of the use of this material.

International Journal of Remote Sensing
Vol. 31, No. 11, 10 June 2010, 3037–3050

Taylor & Francis
Taylor & Francis Group

Topographic normalization for improving vegetation classification in a mountainous watershed in Northern Thailand

LAN CUO*†, JOHN B. VOGLER‡ and JEFFERSON M. FOX§
†Australia Commonwealth Scientific and Industrial Research , Organization (CSIRO), 37 Graham Road, Highett, VIC 3189, Australia
‡Department of Anthropology, University of Hawaii at Manoa, USA
§East-West Center, Honolulu, Hawaii, USA

(*Received 1 October 2006; in final form 27 October 2008*)

Downloaded By: [Fox, Jefferson M.] At: 23:37 20 July 2010

Land cover classifications are adversely affected by shading or topographic effects in mountainous areas in that the spectral properties of an entity in the shade appear to be different from those of the same entity in a sunlit area. Topographic effects can make it especially difficult to distinguish different successional stages of vegetation. The current work uses a simplified topographic normalization method to reduce the topographic effect and to improve land cover classification in a mountainous watershed in northern Thailand. Data used in the study were two Landsat 7 Enhanced Thematic Mapper Plus (ETM+) images acquired on 5 March 2000 and 7 February 2002, a digital elevation model, and Global Positioning Systems (GPS) ground truth data collected in July 2002 consisting of geographic location (latitude/longitude), feature information and ground reference photographs. A supervised land cover classification was conducted on original and normalized images. In general, the classification accuracy of the different successional stages of vegetation was improved in the normalized images.

1. Introduction

Rough terrain generates variable solar incidence angles and exitance angles. These variable angles cause variability in the reflected radiation received by the sensor (Holben and Justice 1980). In a mountainous area, ground features that are the same may appear to have different reflectances due to the rough terrain, especially in near-infrared and mid-infrared bands, which poses problems in land cover classification. Consequently, the misrepresentation of land cover affects hydrological models and land surface models in which land cover maps play an important role.

The near-infrared band (Landsat 7 Enhanced Thematic Mapper Plus (ETM+) band 4) combined with other bands are usually used to identify and classify vegetation because of the higher reflectance of vegetation in band 4 compared with other ground features. Vigorously growing vegetation has even higher reflectance than other types of vegetation in near- and middle-infrared bands (Leprieur *et al.* 1988). However, in Landsat 7 ETM+ imagery, near infrared reflectance of all ground features is depressed by shade. In the shade, vigorously growing vegetation has similar spectral properties to older growing vegetation. This topographic effect thus poses difficulty in distinguishing young, vigorously growing vegetation from more mature vegetation

*Corresponding author. Email: cuol@u.washington.edu

International Journal of Remote Sensing
ISSN 0143-1161 print/ISSN 1366-5901 online © 2010 Taylor & Francis
http://www.tandf.co.uk/journals
DOI: 10.1080/01431160903154333

when using Landsat 7 ETM+ imagery, especially in imagery covering a tropical mountainous region.

In mountainous northern Thailand, swidden agriculture (shifting cultivation) is practiced by upland farmers (Fox *et al.* 1995, Geist and Lambin 2001). Local people cut trees, burn the cut area, and then plant dry land rice, corn and vegetables for a few years. When the fertility of the land decreases, the land is abandoned and farmers shift to another piece of land. The abandoned land gradually changes from agricultural land to fallow, to young secondary forest and, ultimately, advanced secondary forest if the abandonment period is sufficiently long. Different stages of successional vegetation commonly co-exist in these settings. To improve classification of different stages of successional vegetation in northern Thailand, it is necessary to reduce shading effects, or topographic effects.

Various methods have been used to correct topographic effects. Elumnoh and Shrestha (2000), for example, used a band ratio approach without considering physical processes; others have used a statistical-empirical correction derived from an original image and an illumination model generated from a digital elevation model (DEM) (Smith *et al.* 1980, Teillet *et al.* 1982, Civco 1989, Naugle and Lashlee 1992, Baban and Yusof 2001); still others have combined a DEM with an atmospheric correction model (Yang *et al.* 1993, Fashi *et al.* 2000); finally Welch *et al.* (2002) combined air photo interpretation and geographic information system (GIS).

Colby (1991) compared the band ratio method and a backwards radiance correction transformation (BRCT) model using a non-Lambertian assumption and a Minnaert constant in Rocky Mountain National Park, Colorado, US. The study found that the BRCT model was a more successful technique for reducing the topographic effect. Itten and Meyer (1993) found that through the combination of atmospheric and slope-aspect correction, classification accuracy of forest versus non-forest of almost 90% could be achieved in mountainous pre-Alps in central Switzerland with the aid of high quality ground truth. They found that atmospheric correction alone did not improve the classification significantly compared with using only a slope-aspect correction. Meyer *et al.* (1993) tested the pure statistical-empirical correction, the classical cosine (Lambertian) correction, the Minnaert correction, and the C-correction in mountainous pre-Alps in central Switzerland without considering atmospheric effects. High quality ground truth data and a fine resolution DEM allowed them to precisely assess the applicability of the four methods. They demonstrated that the classical cosine method resulted in greater error than the other three methods, and the differences among the results of the other three methods were small. Ekstrand (1996) developed two models of the Minnaert correction, one based on Minnaert constants changing with the cosine of the incidence angle, and the other based on an empirical relationship to derive Minnaert constants. Ekstrand found that both models gave satisfactory results although the empirical model performed better in specific areas in south-western Sweden.

An extensive literature search found no topographic correction studies in Thailand except for Elumnoh and Shrestha (2000). The objectives of this study were to reduce topographic effects using an appropriate method and to improve land cover classifications of a mountainous area in northern Thailand. The final product was used as an input to the distributed hydrological soil vegetation model (DHSVM) to study land cover change effects on local hydrology (Cuo et al. 2006, 2008).

Downloaded By: [Fox, Jefferson M.] At: 23:37 20 July 2010

2. Study area

The study area is located in the mountainous region of northern Thailand (19° 1′ 12″ N–19° 10′ 12″ N, and 98° 37′ 12″ E–98° 46′ 12″ E). The area lies within the Indian south-west summer monsoon and north-east Asian winter monsoon climate system, and is also the location of the headwaters of the major river systems of South-east Asia (figure 1). The climate is characterized by alternating dry and wet seasons with most rainfall occurring between May and November.

The focus of this study was a watershed located within the above latitude and longitude region. Figure 1 shows the DEM of the study watershed, located in the Chiang Mai Province. The area of the watershed is approximately 107 km^2. Elevation ranges from around 680 m to 1776 m, and slope ranges approximately from 0° to 44° in the watershed. The major forest types include a lowland deciduous forest association (deciduous dipterocarp, bamboo, deciduous forest and mixed evergreen deciduous forest) and upland evergreen forest. Land cover in the study area can be classified into tilled fields, with more bare soil and less vegetation; dry rice fields, with more short vegetation and less bare soil; fallow fields, with dense grass, shrub or mature corn; orchard and tea fields, with partial soil exposure; young secondary forest; and advanced secondary forest.

3. Data

The data used in this study consisted of two Landsat 7 ETM+ images:

1. 5 March 2000, path 131, row 047, sun elevation = 52.34°, sun azimuth = 128.32°;
2. 7 February 2002, path 131, row 047, sun elevation = 44.53°, sun azimuth = 136.68°;

Both images were radiometrically and geometrically corrected when received. The 7 February 2002 image was co-registered to the 5 March 2000 image with a sub-pixel precision (root mean square error (RMSE) < 0.5). Both images were subset to the latitude and longitude region mentioned above.

The 30-m resolution DEM used in the study has the same resolution as the satellite imagery in the visible bands, as suggested by Itten and Meyer (1993). The DEM was generated from a 1:50 000 scale topographic map (Royal Thai Survey) with 20-m interval contours, which were digitized by Chiang Mai University. The horizontal positional accuracy and elevation values of the digitized contours were confirmed by overlaying the contours on a scanned, georeferenced topographic map and systematically comparing the two sources for any discrepancies for the area. The vertical accuracy of the mapped contours was not provided on the source map. DEM generation was accomplished using the standard TopoGRID interpolation tool in ArcINFO software that is specifically designed for creating hydrologically correct surfaces from contour data.

In July 2002, a field survey was conducted in the study watershed to collect ground truth reference data. Local people were interviewed at most global positioning system (GPS) sites to collect the information on seasonal land cover change and land cover change over the previous 2-year period. Seasonal land cover change information is used for supervised land cover classification because two images were obtained in dry season while field survey was conducted in wet season. Approximately 100 GPS reference locations were used in the current study. Differential correction was not

Downloaded By: [Fox, Jefferson M.] At: 23:37 20 July 2010

COLOUR FIGURE

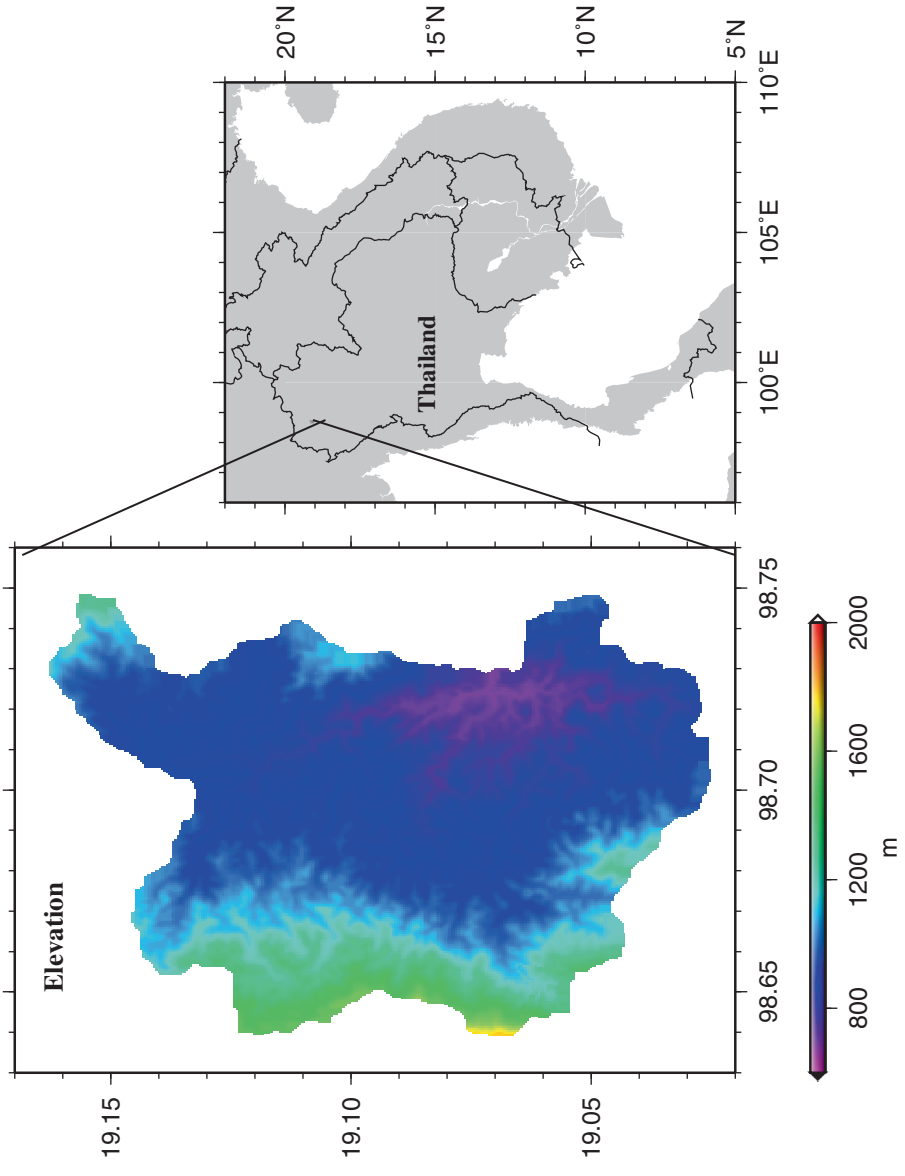

Figure 1. Geographic location 1 cm : 0.04 degree and topographic map of the study site.

Downloaded By: [Fox, Jefferson M.] At: 23:37 20 July 2010

applied to all GPS position measurements due to errors in some base station data acquired in Chiang Mai. Differentially corrected GPS position measurements had an accuracy of 3–5 m. To improve mapping accuracy and in lieu of differential correction methods for the remaining locations (i.e. those with bad or missing base station data), at each reference location, a minimum of 180 GPS position measurements were recorded (3 minutes of recording at one position per second) and averaged, with a maximum allowed position dilution of precision (PDOP) value of 2.0. As PDOP is a multiplicative factor in determining total position error, it was imperative to keep this maximum allowed PDOP value as low as possible without adding substantial recording time to the data collection process. For the Geoexplorer GPS units we used, single position measurements can be expected to provide 10–15 m accuracy 95% of the time (some tests have reported 7–10 m accuracy 95% of the time). The averaging of multiple position measurements at a single location provides improved position accuracy over single position measurements (and their expected accuracies) alone. For some open canopy locations, 200 position measurements were recorded at most, and it should be noted that at several closed canopy locations it was only feasible to record 20–30 position measurements. All GPS data, satellite imagery, and DEM were georeferenced to Universal Transverse Mercator (UTM) coordinate system and world geodetic system 1984 (WGS84) datum.

Downloaded By: [Fox, Jefferson M.] At: 23:37 20 July 2010

4. Methods

4.1 *Reduction of topographic effects*

In Elumnoh and Shrestha (2000), which was the only study conducted in mountainous Thailand, the composite image of band 7 and band 5 ratio, normalized difference vegetation index (NDVI), the first principal component and DEM generated the highest land cover classification accuracy compared to the other 11 feature sets in central Thailand (see their table 2). Following the procedure of Elumnoh and Shrestha (2000), the composite images on two dates were generated. As a result, small patches of shade were reduced, but larger patches of shade remained. The Lambertian correction in the ERDAS IMAGINE software, or classical cosine correction, was also applied. The resulting images exhibited larger variance of brightness values than the original images. The topographic effect was over-corrected, mainly due to the rough surface on mountain slope facets, which was not in accord with the Lambertian smooth surface assumption.

The Minnaert correction is a modification of the Lambertian correction. Ekstrand (1996) used a linear regression method to calculate the Minnaert constant k_λ with the following equations:

$$k_\lambda = \frac{\overline{y_{ij}}_\lambda - \overline{b_{ij}}_\lambda}{\overline{x_{ij}}} \tag{1}$$

$$y_{ij\lambda} = \ln(L_{t\lambda} \cos e) \tag{2}$$

$$x_{ij} = \ln\left({(\cos a \cos e)}/{\cos z} \right) \tag{3}$$

$$b_{ij\lambda} = \ln(L_{h\lambda}), \tag{4}$$

where i and j are row and column numbers of a pixel; k_λ is the Minnaert constant for wavelength λ; $L_{t\lambda}$ is the radiance observed over the inclined terrain for wavelength λ; e is the surface normal zenith angle or terrain slope; a is solar incidence angle, the angle between the surface normal and the solar beam; z is solar zenith angle; and $L_{h\lambda}$ is the radiance over a horizontal surface for wavelength λ.

The normalized radiance $L_{N\lambda}$ for a horizontal surface when the sun is at the zenith, i.e. $a = e = 0$, is then calculated by:

$$L_{N\lambda} = L_\lambda / \left(\cos^{k_\lambda - 1} e \cos^{k_\lambda} a\right) \tag{5}$$

where L_λ is given as the digital number at an angle e and a in each band.

When following the above procedure, it was found that $x_{ij} = \ln\left(\left(\cos a \cos e\right)/\cos z\right)$ was not normally distributed, violating one assumption of linear regression technique.

After further testing, it was found that a modification of the method proposed by Civco (1989) effectively reduced the shading effects. Generally, there are four steps in Civco's method. We modified the third step. The following are the procedures used in the study:

1. The DEM and solar azimuth and elevation angles provided in the imagery metadata file were used to generate illumination models for the two dates. Illumination models were scaled over the 8-bit brightness range (0–255 grey level).
2. The first stage linear transformation of each of the original ETM+ bands was then performed to derive topographically normalized images, using

$$R'_{ij\lambda} = R_{ij\lambda} + \left(R_{ij\lambda} \frac{U - u_{ij}}{U}\right), \tag{6}$$

   where $R'_{ij\lambda}$ is the first stage normalized radiance data for pixel (i, j) in band λ, $R_{ij\lambda}$ is the raw radiance data for pixel (i, j) in band λ, U is the mean value for the entire scaled (0–255) illumination values, and u_{ij} is the scaled (0–255) illumination value for pixel (i, j).
3. To further correct the topographic effect, an empirically-derived calibration coefficient was determined for each band by

$$C_\lambda = \frac{1}{2}\left(\frac{\mu_\lambda - N_\lambda}{(\mu_\lambda - N_\lambda) - (\mu_\lambda - N'_\lambda)} + \frac{\mu_\lambda - S_\lambda}{(\mu_\lambda - S_\lambda) - (\mu_\lambda - S'_\lambda)}\right), \tag{7}$$

   where C_λ is the topographic correction coefficient for band λ; μ_λ is the overall digital number mean for band λ; N_λ is the mean on northern slopes of raw data in each band; N'_λ is the mean on northern slopes after the first stage normalization; S_λ is the mean on southern slopes of raw data in each band; S'_λ is the mean on southern slopes after the first stage normalization. Our method varied from Civco (1989) in terms of how we defined these parameters. Civco (1989) related parameters C_λ, μ_λ, N_λ, N'_λ, S_λ, and S'_λ, to specific land covers, whereas we related these parameters simply to the values of each band in this study. This simplification is legitimate because land cover classes on satellite images were unknown before land cover classification. Thus, the modification is just a simplification of Civco's original method in that the knowledge of land cover types is not needed beforehand.

Downloaded By: [Fox, Jefferson M.] At: 23:37 20 July 2010

4. The second stage linear transformation with correction coefficients was used to further correct the topographic effect, using

$$R''_{ij\lambda} = R_{ij\lambda} + \left(R_{ij\lambda} \times \frac{U - u_{ij}}{U} C_\lambda \right), \tag{8}$$

where $R''_{ij\lambda}$ is the second stage normalized radiance data.

4.2 *Land cover classification*

Supervised land cover classification was conducted using GPS data, field notes and ground reference photographs. Approximately 50 GPS points were used to select training areas and generate class signatures, and 53 GPS points were used to assess the land cover classification accuracy.

The Mahalanobis distance supervised land cover classification was applied to the original images and normalized images on both dates, resulting in four land cover maps. Due to 1- to 2-pixel misalignment between the images and GPS data points, liberal accuracy analysis was conducted on the land cover maps. An area of 3 × 3 pixels surrounding a GPS location was used in the accuracy analysis. Land cover change within the 2-year period and due to seasonality was considered during classification and accuracy assessment based on field survey.

5. Results and discussion

The topographic correction coefficient C_λ is specific to each image and each band, and a unique value must be generated for each date and each ETM+ band. Tables 1 and 2 list C_λ and the parameter values used to calculate it for both images on two dates. The tables demonstrate the large differences in average brightness values between northern and southern slopes, especially in the near infrared, and two mid-infrared bands

Table 1. Calculation of C_λ to be used in the second stage normalization for the 5 March 2000 image.

Band	μ_λ	N_λ	N'_λ	S_λ	S'_λ	C_λ
1	70.57	70.27	75.15	71.37	56.76	0.06
2	54.45	53.81	59.29	56.12	44.49	0.13
3	45.03	44.26	46.95	47.06	37.26	0.25
4	72.17	70.13	74.37	77.33	61.32	0.40
5	74.74	71.35	75.25	83.50	66.38	0.69
7	39.74	37.96	39.81	44.36	35.08	0.73

Table 2. Calculation of C_λ to be used in the second stage normalization for the 7 February 2002 image.

Band	μ_λ	N_λ	N'_λ	S_λ	S'_λ	C_λ
1	54.83	54.44	58.03	55.93	44.32	0.10
2	42.62	41.72	44.17	45.02	35.54	0.31
3	33.22	32.27	33.96	35.73	28.13	0.45
4	67.21	64.03	67.44	75.42	59.66	0.73
5	62.72	58.92	61.73	72.61	57.53	1.00
7	32.10	30.35	31.61	36.68	28.87	0.99

Downloaded By: [Fox, Jefferson M.] At: 23:37 20 July 2010

(bands 4, 5, 7, respectively). In the original images, southern slopes have higher average brightness values than northern slopes. After the first stage linear transformation, northern slopes have higher average brightness values than southern slopes.

Figures 2 and 3 are composite images of bands 1, 2, and 3 for original images and normalized images on 5 March 2000, respectively. The image collected on 7 February 2002 basically has the similar results and it is not shown here. Figure 2 depicts the topographic effect in the original ETM+ images. The magnitude of the topographic effect is apparent in the original data. Areas of shade from rough terrain are located throughout the images and are particularly visible in the southern and eastern portions of the scenes. Figure 3 shows that the topographic effect has been significantly reduced after the second stage normalization, while preserving the overall spectral properties of the scene. This observation is supported by the data presented in Table 3 which shows that the overall means of the scenes before and after the second stage normalization are close, while the variances of the overall scenes slightly decrease after second stage normalization.

Land cover classes with small areal extents may be under-represented by GPS data due to their small area and difficult access. In the current study area, under-represented land class is tea/fruit fields. However, since the majority of the land cover classes in the study area are dry rice field, fallow field, advanced secondary forest and young secondary forest, which are represented well by GPS data, the accuracy test for the major land classes was considered reasonable, and the accuracy analysis was focused on the major land cover types.

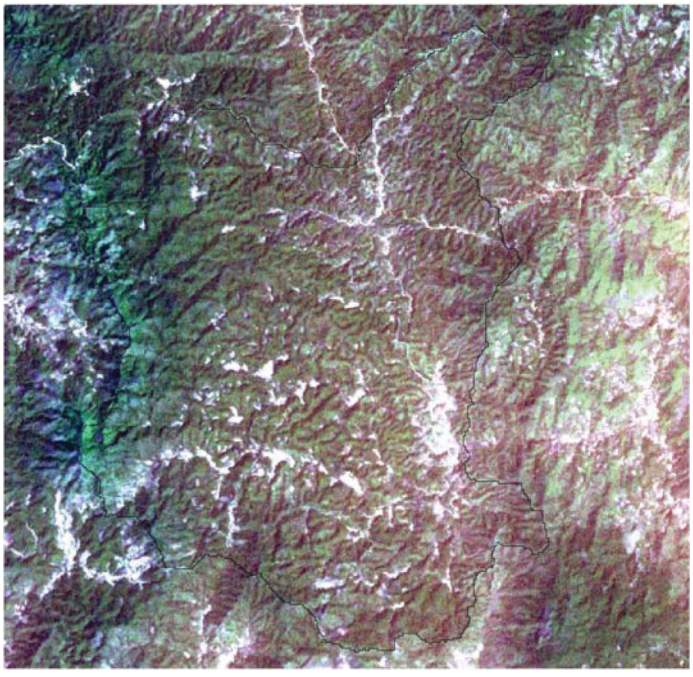

COLOUR FIGURE

Figure 2. Original composite image from bands 1, 2 and 3 on 5 March 2000 for the study area in northern Thailand.

Downloaded By: [Fox, Jefferson M.] At: 23:37 20 July 2010

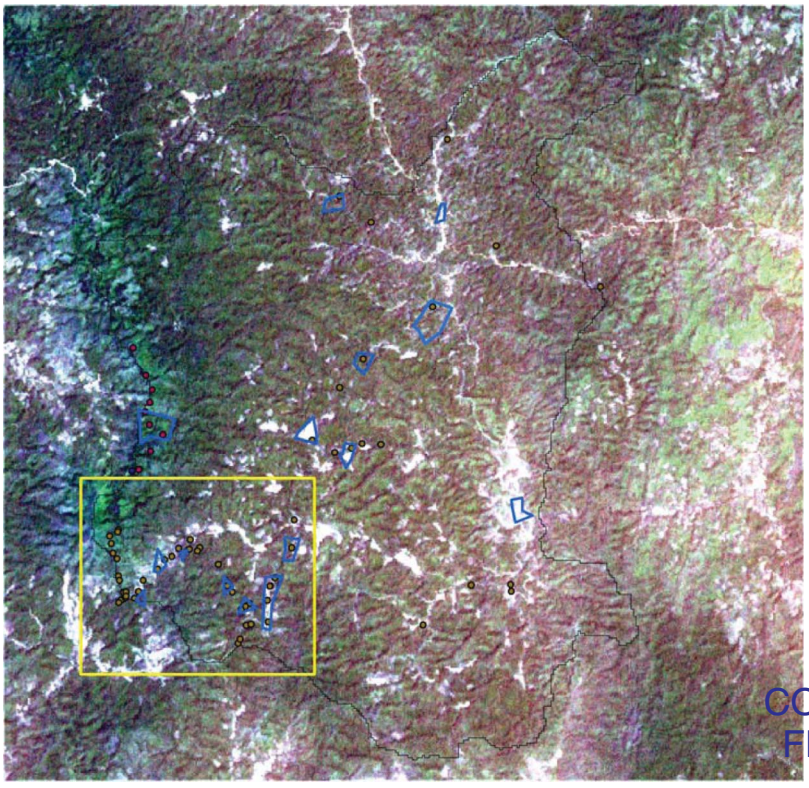

COLOUR FIGURE

Figure 3. Normalized composite image from bands 1, 2 and 3 on 5 March 2000 for the study area. The dots are selected GPS points (different colours represent different dates that the points were collected). Blue polygons are the selected training areas (areas of interest). Validation sites are located in the yellow rectangle.

Table 3. Mean and standard deviation for the entire scene for four images on two dates.

	5 March 2000 image				7 February 2002			
	Original		Normalized		Original		Normalized	
Band	Mean	SD	Mean	SD	Mean	SD	Mean	SD
1	70.57	3.39	70.07	3.32	54.83	3.52	54.30	3.38
2	54.45	3.98	53.92	3.69	42.62	4.94	41.99	4.48
3	45.03	6.67	44.45	6.41	33.22	7.10	32.52	6.68
4	72.17	10.00	71.26	8.69	67.21	12.82	65.60	10.64
5	74.74	17.91	73.16	16.01	62.72	18.40	60.38	15.91
7	39.74	13.05	38.66	12.18	32.10	11.46	30.80	10.58

Mean = overall scene mean ($n = 292\,617$ pixels)
SD = overall scene standard deviation

Table 4 shows that user's accuracy increased for dry rice fields, tilled fields, fallow fields, young secondary forest, and advanced secondary forest after normalization of the 5 March 2000 image. Producer's accuracy increased for dry rice fields, tilled fields, fallow fields, and young secondary forest after normalization. Because tea/fruit fields

Downloaded By: [Fox, Jefferson M.] At: 23:37 20 July 2010

Table 4. Error matrix of land cover classification for 5 March 2000 original image and normalized image.

	Producer's accuracy (%)		User's accuracy (%)	
Class name	Original	Normalized	Original	Normalized
Dry rice field with short grass	63	100	50	73
Tilled field with more bare soil	83	100	56	100
Fallow field with high grass	35	90	78	90
Tea and fruit trees with open ground	100	100	100	100
Advanced secondary forest	90	90	43	75
Young secondary forest	25	38	67	100

occupy only a small portion in the entire study area, and only a few GPS positions are associated with them, the classification accuracy of tea/fruit field is probably overestimated. But again, the focus here is on the major land classes. After normalization, advanced secondary forest was better classified than in the original image. The classification of young secondary forest appears to be more difficult since after the normalization the producer's accuracy was increased by only 13%. Dry rice fields and fallow fields have fairly good classification after normalization.

Table 5 shows that on the 7 February 2002 image, the producer's accuracy increased for dry rice fields, fallow fields, young and advanced secondary forest. User's accuracy for dry rice fields, fallow fields, young and advanced secondary forest also increased. Although the classification process suffered from the small quantity of the GPS reference data, results of the available data do show the improvement in the classifications. As Kawata *et al.* (1988) pointed out, the topographic effect could not be removed completely from severely shadowed areas such as deep valleys. These remaining shaded areas in both normalized images appear to be linear in shape (see figure 3 for the 5 March 2000 image). Since sun elevation angle on 7 February 2002 was lower than that on 5 March 2000, the deeply shaded area was larger on the 7 February 2002 image than on the 5 March 2000 image. The error matrices of validation points for the 5 March 2000 original and normalized images are shown in tables 6 and 7.

Overall accuracy for the 5 March 2000 original image was 55%, and it was increased to 85% after normalization. The Kappa statistic was 0.44 for the original image, and it increased to 0.81 after normalization for the 2000 image. Accuracy for the 7 February 2002 original image was 51%, and the Kappa statistic was 0.35. Accuracy for the 7

Table 5. Error matrix of land cover classification for 7 February 2002 original image and normalized image.

	Producer's accuracy (%)		User's accuracy (%)	
Class name	Original	Normalized	Original	Normalized
Dry rice field with short grass	50	100	63	77
Tilled field with more bare soil	—	—	—	—
Fallow field with high grass	50	75	57	92
Tea and fruit trees with open ground	—	—	—	—
Advanced secondary forest	69	92	39	92
Young secondary forest	36	100	83	100

Downloaded By: [Fox, Jefferson M.] At: 23:37 20 July 2010

Downloaded By: [Fox, Jefferson M.] At: 23:37 20 July 2010

Table 6. Error matrix of validation points for the 5 March 2000 normalized image.

	Reference data							
Classified data	Unclassified	Dry rice field	Tilled field with more bare soil	Fallow field with high grass	Tea and fruit trees with open ground	Advanced secondary forest	Young secondary forest	Row total
Unclassified data	0	0	0	0	0	0	0	0
Dry rice field	0	8	0	2	0	1	0	11
Tilled field with more bare soil	0	0	6	0	0	0	0	6
Fallow field with high grass	0	0	0	18	0	0	2	20
Tea and fruit trees with open ground	0	0	0	0	1	0	0	1
Advanced secondary forest	0	0	0	0	0	9	3	12
Young secondary forest	0	0	0	0	0	0	3	3
Column total	0	8	6	20	1	10	8	53

Downloaded By: [Fox, Jefferson M.] At: 23:37 20 July 2010

Table 7. Error matrix of validation points for 5 March 2000 original image.

	Reference data							
Classified data	Unclassified	Dry rice field	Tilled field with more bare soil	Fallowfield with high grass	Tea and fruit trees with open ground	Advanced secondary forest	Young secondary forest	Row total
Unclassified data	0	0	0	0	0	0	0	0
Dry rice field	0	5	0	4	0	1	0	10
Tilled field with more bare soil	0	3	5	1	0	0	0	9
Fallow field with high grass	0	0	0	7	0	0	2	9
Tea and fruit trees with open ground	0	0	0	0	1	0	0	1
Advanced secondary forest	0	0	0	8	0	9	4	21
Young secondary forest	0	0	1	0	0	0	2	3
Column total	0	8	6	20	1	10	8	53

February 2002 normalized image was 91% and the Kappa statistic was 0.87. In general, it can be seen that the simplified topographic normalization method improved the classification of the two images.

6. Conclusion

Using a simplified normalization method, the topographic effect in the study area was reduced while preserving the spectral properties of the original imagery in general. Compared to the original image classification for the two dates, normalized images produced better land cover classification as seen from overall accuracy and Kappa statistics.

Due to some limitations in the GPS data collecting process, the quality and quantity of the GPS ground truth data used in the current study were not ideal. There are a few things that could be improved in order to have better land cover classification, e.g. establishment of a good connection with one or more local official base stations that collect and deliver reliable differential correction data, close alignment of seasonality and timing of image acquisition and GPS collection, collection of wide spread GPS data throughout the study area, and sufficient representation of all land classes in GPS reference data.

Acknowledgement

This material is based upon work supported by the US National Science Foundation under Grant No. EAR-0000546.

References

Baban, S.M.J. and Yusof, K.W., 2001, Mapping land use/cover distribution on a mountainous tropical island using remote sensing and GIS. *International Journal of Remote Sensing*, **22**, pp. 1909–1918.

Civco, D.L, 1989, Topographic normalization of Landsat thematic mapper digital imagery. *Photogrammetric Engineering and Remote Sensing*, **55**, pp. 1303–1309.

Colby, J.D., 1991, Topographic normalization in rugged terrain. *Photogrammetric Engineering and Remote Sensing*, **57**, pp. 531–537.

Cuo, L., Giambelluca, T.W., Ziegler, A.D. and Nullet, M.A., 2006, Use of the distributed hydrology soil vegetation model to study road effects on hydrological processes in Pang Khum Experimental Watershed, northern Thailand. *Forest Ecology and Management*, **224**, pp. 81–94.

Cuo, L., Giambelluca, T.W., Ziegler, A.D. and Nullet, M.A., 2008, The roles of roads and agricultural land use in alternating hydrological processes in Nam Mae Rim watershed, northern Thailand. *Hydrological Processes*, **22**, pp. 4339–4354.

Ekstrand, S., 1996, Landsat TM-based forest damage assessment: correction for topographic effects. *Photogrammetric Engineering and Remote Sensing*, **62**, pp. 151–161.

Elumnoh, A. and Shrestha, R.P., 2000, Application of DEM data to Landsat image classification: evaluation in a tropical wet-dry landscape of Thailand. *Photogrammetric Engineering and Remote Sensing*, **66**, pp. 297–304.

Fahsi, A., Tsegaye, T., Tadesse, W. and Coleman, T., 2000, Incorporation of digital elevation models with Landsat-TM data to improve land cover classification accuracy. *Forest Ecology and Management*, **128**, pp. 57–64.

Fox, J., Krummel, J., Yarnasarn, S., Ekasingh, M. and Podger, N., 1995, Land use and landscape dynamics in northern Thailand: assessing change in three upland watersheds. *Ambio*, **24**, pp. 328–334.

Downloaded By: [Fox, Jefferson M.] At: 23:37 20 July 2010

Geist, H.J. and Lambin, E.F., 2001, What drives tropical deforestation: a meta-analysis of proximate and underlying causes of deforestation based on subnational case study evidence, LUCC report, series No.4, LUCC, IHDP, GLOBAL change, IGBP, CIACO, Louvain-la-Neuve.

Holben, B.N. and Justice, C.O., 1980, The topographic effect on spectral response from nadir-pointing sensors. *Photogrammetric Engineering and Remote Sensing*, **46**, pp. 1191–1200.

Itten, K.I. and Meyer, P., 1993, Geometric and radiometric correction of TM data of mountainous forested areas. *IEEE Transactions on Geoscience and Remote Sensing*, **31**, pp. 764–770.

Kawata, Y., Ueno, S. and Kusaka, T., 1988, Radiometric correction for atmospheric and topographic effects on Landsat MSS images. *International Journal of Remote Sensing*, **9**, pp. 729–748.

Leprieur, C.E., Durand, J.M. and Peyron, L.L., 1988, Influence of topography on forest reflectance using Landsat thematic mapper and digital terrain data. *Photogrammetric Engineering and Remote Sensing*, **54**, pp. 491–496.

Meyer, P., Itten, K.I., Gellenberger, T., Sandmeier, S. and Sandmeier, R., 1993, *ISPRS Journal of Photogrammetry and Remote Sensing*, **48**, pp. 17–28.

Naugle, B.L. and Lashlee, J.D., 1992, Alleviating topographic influences on land-cover classifications for mobility and combat modeling. *Photogrammetric Engineering and Remote Sensing*, **58**, pp. 1217–1221.

Smith, J.A., Lin, T.L. and Ranson, K.J., 1980, The Lambertian assumption and Landsat data. *Photogrammetric Engineering and Remote Sensing*, **46**, pp. 1183–1189.

Teillet, P.M., Guindon, B. and Goodenough, D.G., 1982, On the slope-aspect correction of multispectral scanner data. *Canadian Journal of Remote Sensing*, **8**, pp. 84–106.

Welch, R., Madden, M. and Jordan, T., 2002, Photogrammetric and GIS techniques for the development of vegetation databases of mountainous areas: Great Smoky Mountains National Park. *ISPRS Journal of Photogrammetry and Remote Sensing*, **57**, pp. 53–68.

Yang, C., Uruya, W. and Cristian, P., 1993, Correction radiometrique sur les donees satellitaires en zone de reflief: modelisation et application. In *Teledetection et Cartgraphie*, AUPELF-UREF (Ed.), pp. 65–80 (Quebec, Canada: Les Presses de l'Universite de Quebec).

Downloaded By: [Fox, Jefferson M.] At: 23:37 20 July 2010